

A sub-basin scale dust plume source frequency inventory for southern Africa, 2005–2008

Kathryn J Vickery,¹ Frank D Eckardt,¹ and Robert G Bryant²

Received 12 July 2013; revised 4 September 2013; accepted 14 September 2013.

[1] We present a dust plume source inventory for southern Africa. In order to locate and track the local, short-lived plume events, source and frequency data have been derived from Meteosat Second Generation (MSG) thermal infrared composite data (4 km data using 8.7, 10.8, and 12.0 μm) and Moderate Resolution Imaging Spectroradiometer (MODIS) visible composite data (0.25 km data utilizing 0.620 – 0.670 μm , 0.545 – 0.565 μm , and 0.459 – 0.479 μm). Between January 2005 and December 2008, a total of 328 distinct daytime dust plumes more than 10 km in length were detected. These plumes were attributed to 101 distinct point sources, consisting largely of ephemeral inland lakes, coastal pans as well as dry river valleys in Namibia, Botswana, and South Africa. These data also provided sub-basin scale source observations for large basins such as Etosha and Makgadikgadi Pans. **Citation:** Vickery, K. J., F. D. Eckardt, and R. G. Bryant (2013), A sub-basin scale dust plume source frequency inventory for southern Africa, 2005–2008, *Geophys. Res. Lett.*, *40*, doi:10.1002/grl.50968.

1. Introduction

[2] The emission of dust (mineral aerosol) can play an important role in the land-atmosphere-ocean system [e.g., Washington *et al.*, 2009; Okin *et al.*, 2011; Ravi *et al.*, 2011; Knippertz and Todd, 2012] through interaction with biogeochemical cycles [e.g., Mahowald *et al.*, 2009; Gabric *et al.*, 2010; Schulz *et al.*, 2012], and direct and indirect radiative forcing of the atmosphere [e.g., Mahowald, 2011; Skiles *et al.*, 2012]. The relative impact of dust in the Earth's system depends on characteristics such as particle size, shape, and mineralogy [e.g., Mahowald *et al.*, 2009; Kok, 2011]. Whilst these characteristics can change during dust transport [e.g., Carslaw *et al.*, 2010], they are initially determined by the terrestrial sources from which particles are entrained [e.g., Kohlfeld and Tegen, 2007]. Our principal means of predicting the impacts of dust emission on future weather and climate are through the use of numerical models [e.g., Mahowald *et al.*, 2011; Shao *et al.*, 2011; Knippertz and Todd, 2012].

Additional supporting information may be found in the online version of this article.

¹Department of Environmental and Geographical Science, University of Cape Town, Rondebosch, Cape Town, South Africa.

²Department of Geography, University of Sheffield, Sheffield, S. Yorkshire, UK.

Corresponding author: F. D. Eckardt, Department of Environmental and Geographical Science, University of Cape Town, Rondebosch, Cape Town 7701, South Africa. (frank.eckardt@uct.ac.za)

©2013. American Geophysical Union. All Rights Reserved.
0094-8276/13/10.1002/grl.50968

[3] At the global scale, remote sensing has been instrumental in allowing sources of dust and their behavior to be identified. TOMS (Total Ozone Mapping Spectroradiometer) and other global aerosol index (AI)-based studies [e.g., Prospero *et al.*, 2002; Bryant, 2003; Washington *et al.*, 2003; Bryant *et al.*, 2007] have produced dust maps which emphasize aerosol dispersion, rather than explicit dust origin. Engelstaedter and Washington [2007] made a significant advance on the foundational TOMS-based studies by Prospero *et al.* [2002] and Washington *et al.* [2003] by adding surface gustiness in their global analyses. The Engelstaedter and Washington [2007] study established 131 global hotspots, six of which were in southern Africa, most of which due to the coarse resolution remained largely unspecified domains with limited geomorphological understanding of sources. Even with higher resolution products, Ginoux *et al.* [2012], who presented a synthesis of global-scale high-resolution (0.1°) dust source locations based on Moderate Resolution Imaging Spectroradiometer (MODIS) Deep Blue aerosol measurements [Hsu *et al.*, 2004; Hsu *et al.*, 2006], still did not improve upon the specifications of southern African sources. It is clear that inherent seasonal and diurnal dust emission variations along with the spatial heterogeneity of dust sources in global and mesoscale models are poorly constrained due to inexact source allocation and quantification [e.g., Zender *et al.*, 2003; Mahowald *et al.*, 2007; Bullard *et al.*, 2011]. Regional observations utilizing higher-temporal and spatial resolution data have been more successful in deriving information pertaining to the dust sources and activation frequency. For example, studies using Meteosat Second Generation (MSG)-SEVIRI (Spinning Enhanced Visible and Infrared Imager) in northern Africa point toward a series of approaches that may be taken to match remote sensing data of dust events or more generally “dustiness” to the temporal signature of meteorological emission drivers [see Schepanski *et al.*, 2007; Ashpole and Washington, 2012]. Outside of the Sahara dust belt, very few inventories of dust sources at the sub-basin scale exist. Nevertheless, it is apparent that the detection of spatially discrete and intermittent sources can be undertaken using moderate resolution polar-orbiting data, e.g., SeaWiFS (Sea-viewing Wide Field-of-view Sensor) [Eckardt and Kuring, 2005], MODIS [Bullard *et al.*, 2008; Baddock *et al.*, 2009], and a combination of GOES (Geostationary Operational Environmental Satellite) and MODIS [Lee *et al.*, 2009; Rivera Rivera *et al.*, 2010].

[4] Initial southern African aerosol research had focused on the industrial Highveld, where the role of mineral aerosols was found to be marginal [e.g., Ichoku *et al.*, 2003]. Nevertheless, SAFARI-92 and SAFARI 2000 established a greater understanding of both air-transport patterns and the temporal variability of regional aerosols [e.g., Maenhaut *et al.*, 2002; Ichoku *et al.*, 2003]. These initiatives identified

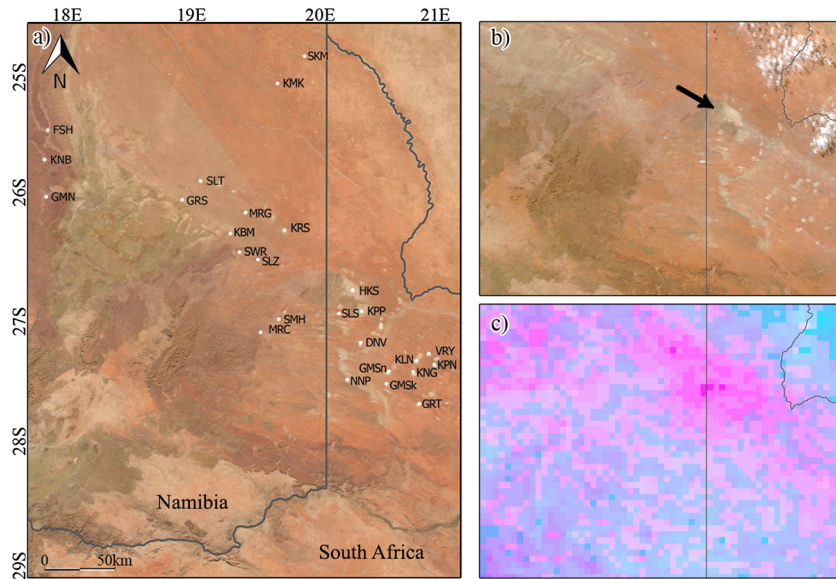


Figure 1. (a) Newly identified active south west Kalahari plume sources seen between 2005 and 2008 depicted in clear MODIS image. Subset 1b) Hakskeenpan (HKS) “true color” plume in MODIS (Terra 07:15 GMT) and 1c) dispersed “pink” dust around HKS later in the day seen in MSG (13:00 GMT) (both 19 May 2007, Julian Day 139). Sources in alphabetical order are: DNV: Donovan se Pan, FSH: Fish River, GMN:Gamanas Pan, GMSk: Gemsbokbrak, GMSn: Gemsbokhoorn, GRS: Grasheuwel Pan, GRT: Groot – Witpan, HKS: Hakskeenpan, KBM: Kuubmaansvlie, KLN: Klein-Aarpan, KMK: Koemkoep, KNB: Kanibes River, KNG: Kongapan, KNP: Koipan, KPP: Koppieskraalpan, KRS: Kiriis Ost Pan, MRC: Marcel Pan, MRG: Morgenzon Pan, NNP: Noenieput, SKM: Skemerhoek Pan, SLS: Soulstraatpan,SLT: Salt Pan, SLZ: Salztal Pan, SMH: Samahaling Pan, SWR: Swartput se Pan, VRY: Vrysoutpan.

that; aerosol loads peak during August and September, include a component of aeolian dust [Piketh *et al.*, 1999], and coincide with the period of significant biomass burning [Abel *et al.*, 2005]. The main sources of the regional mineral aerosol load are from the Etosha Pans in Namibia and the Makgadikgadi Pans in Botswana [Prospero *et al.*, 2002; Washington *et al.*, 2003; Bryant *et al.*, 2007]. These two ephemeral lake basins are amongst the southern hemisphere’s most significant dust sources. The aim of this study is to provide the first unified, subcontinental, and detailed dust plume source location inventory for southern Africa, using a combination of MSG-SEVIRI and MODIS data.

2. Method

[5] Regional observations of dust events and sources outside of the dust belt of the Sahara involve a range of challenges [see Bryant, 2013]. In order to detect spatially and temporally discrete dust events (i.e., plumes) using remote sensing data, it is clear one has to take account of: (i) the varying performance of dust detection algorithms with variable dust thickness, height, and mineralogy [e.g., Baddock *et al.*, 2009] (ii) lags that may exist between the timing of satellite overpass and dust plume emission, (iii) cloud and water vapor effects, and (iv) subjectivity in identifying events and pinpointing dust storm emission locations [e.g., Baddock *et al.*, 2009; Brindley *et al.*, 2012]. To overcome some of these issues, combined use of remote sensing data providing high spatial resolution and high sample frequency was considered [Banks *et al.*, 2013]. We use a similar multisensor approach to Lee *et al.* [2009] and Rivera Rivera *et al.* [2010] by combining MODIS visible composite data (utilizing 0.620 – 0.670 μm , 0.545 – 0.565 μm , and 0.459 – 0.479 μm at 0.25 km) derived

from NASA Terra and Aqua platforms. Terra (~08:30 GMT) and Aqua (~13:30 GMT) orbits provided images with a nadir resolution of 0.25 km representing morning and afternoon conditions. This was combined with data from the SEVIRI instrument on-board the MSG satellite utilizing the Brightness Temperature Difference (BTD) product using the 8.7 μm , 10.8 μm , and 12 μm channels at 4 km resolution. Three daily images representing morning (07:00 GMT), noon (10:00 GMT), and afternoon (13:00 GMT) were extracted. Ackerman [1997] and Baddock *et al.* [2009] provided a comprehensive review of dust detection in the visible and infrared wavelengths also used here, while Schepanski *et al.* [2007] and Brindley *et al.* [2012] provided a summary of the advantages and disadvantages of MSG-SEVIRI BTD algorithm for dust detection. Dust plumes occurring underneath clouds were unlikely to be detected.

[6] In order to build a plume and source location inventory for southern Africa between 2005 and 2008 (Figure 1), images were visually examined for dust plumes. Sequential viewing of MODIS images permitted the identification of plumes due to the obscuring of darker surface features by pale dust. Applying the BTD algorithm to SEVIRI data gave airborne dust plumes a characteristic pink hue which in sequential imagery were also noted to move. Consistent dispersion headings and patterns, as well as the short-lived nature of coherent plume pulses facilitated source identification. On occasions, dispersed haze was evident which was not attributed to a discrete source or cause. However active fires are flagged in the MODIS online product making confusion with dust plumes highly unlikely. Not all plumes were observed to be attached to a source but could still be attributed to likely emission points based on heading and dispersion patterns. Furthermore, the interpreted

Table 1. Dust Plume Source Types for Each of the Five Regions Identified in This Study^a

		Pan	River	Marsh	Mine	Total n	(%)
Makgadikgadi, Botswana	Sources	1				1	
	Plumes	53				53	16
Etosha, Namibia	Sources	2 ^b				2	
	Plumes	32				32	10
Namib Desert, Namibia	Sources	29	39	1 ^c	1 ^d	70	
	Plumes	85	111	6	1	203	61
South West Kalahari, S.Africa, Namibia	Sources	24	2			26	
	Plumes	35	2			37	11
Free State, S. Africa	Sources	2				2	
	Plumes	3				3	1
Total sources	n	58	41	1	1	101	
	(%)	58	40	1	1		
Total plumes	n	208	113	6	1	328	
	(%)	64	34	2	0		

^aPans dominate in terms of sources count (57%) and number of detectable plumes (64%). The Makgadikgadi Pan Complex accounts for 16% of all detectable plumes, which do originate from several clusters in the Sua and Ntwetwe sub-basins. The Namib Desert hosts 70 of the 101 sources producing 62% of all detectable plumes. Ephemeral rivers accounted for more than half of all plume sources in this region.

^bOnanzi Pan was active beyond the main shore of the Etosha Pan and was counted separately.

^cThis marsh represents the interdune oasis in the Lower Hoanib River.

^dThis source is located near the Orange River mouth and could be the result of mining.

transport directions were generally supported by daily synoptic charts. Geo-referenced MODIS and MSG images allowed the position of plume sources to be scrutinized against Landsat imagery and topographic data which helped us to collocate plume sources to specific land surface features. GIS allowed for plume metrics such as timing and length to be captured and enabled dust plume frequency to be compiled.

3. Results and Discussion

3.1. Spatial Observations

[7] Between 2005 and 2008, the multisensor approach detected 328 dust plumes greater than 10 km in length (Table 1). On average, our plumes measured only 96 km and even the longest plumes were only around 400 km long, which generally remained well defined, local in extent, and short lived in nature, lasting for a few hours at most. This along with their limited dispersion pattern made source identification relatively easy. We were therefore able to attribute these plumes to 101 source locations (Supporting Table S1) from five principle source regions (Figure 2 and Supporting Figure S2) which can be ranked by dust plume counts per source as follows: (1) The Makgadikgadi Pan (Botswana) produced 53 distinct plumes on 31 days originating from four ephemeral sub-basins in northern and southern Sua and Ntwetwe Pans. (2) The Etosha Pan region (Namibia) generated 32 dust plumes on 22 days with dominant emissive clusters in the western and eastern sub-basin. (3) The 1500 km long Namibian coastline (Namibia) emitted 203 plumes on 39 days from 70 unique plume sources including pans (sabkhas and playas), ephemeral rivers, wetlands, and possibly a mine. (4) In addition, the 300 km long, south-western Kalahari Pan Belt (South Africa and Namibia), hosted 37 events on 9 days from 24 pans and two associated drainage lines (Figure 1a). (5) The pans of the Free State (South Africa) only yielded three plumes on three separate days from two distinct sources with agriculture possibly also being a contributing factor.

[8] Our source inventory adds considerable detail to the two major dust domains first flagged by TOMS [e.g., Prospero, 1999; Washington *et al.*, 2003]. While confirming the magnitude of Etosha and Makgadikgadi pans [Bryant, 2003; Bryant *et al.*, 2007], this study for the first time identifies persistent sub-basin clusters of sources which are responsible for emissions within these large pans. Furthermore, observations here not only extend the dust plume record for Namib sources, (1972–1995 Space Shuttle photography in Eckardt *et al.* (2001) and 1998–2001 from SeaWiFS in Eckardt and Kuring [2005]) but also add 39 previously unidentified source points to the inventory. The Kuiseb River was first identified as highly productive in Eckardt and Kuring [2005], an observation we can now confirm with the Kuiseb accounting for 20% of all Namibian River plumes seen here. Vickery and Eckardt [2013] have recently examined the controls which could make this the dustiest river in southern Africa. Our observations also captured active pans in the south-western Kalahari; a region tentatively flagged in an earlier TOMS product [Engelstaedter and Washington, 2007] with Hakskeenpan in South Africa being its largest and most productive source (6 plumes). Despite the vast number of pans in the Karoo and Free State, and known dust events having been observed at ground level [Holmes *et al.*, 2008], this region produced only a few detectable plumes in our imagery for the observation period.

[9] In terms of plume frequency over the study period, our study compares to source inventories from the Chihuahuan Desert, Lake Eyre Basin (LEB), and the Sahara [Bullard *et al.*, 2011] (Table 1). The multisensor approach used here has identified large and small pans, some of which are only a few km² in size, as the most prolific regional sources of plumes (57%), with the remaining attributed to rivers and wetlands including the Hoanib Oasis. This trend was consistent across data types, with MSG also resulting in the attribution of ~50% of all sources as pans; accounting for 52 of the 65 events which is more than elsewhere (Chihuahuan Desert Pans, 30%; LEB, 11%; and Sahara, 3%). Clearly, different land surfaces play different roles in the dust cycle across regions, which has further implications

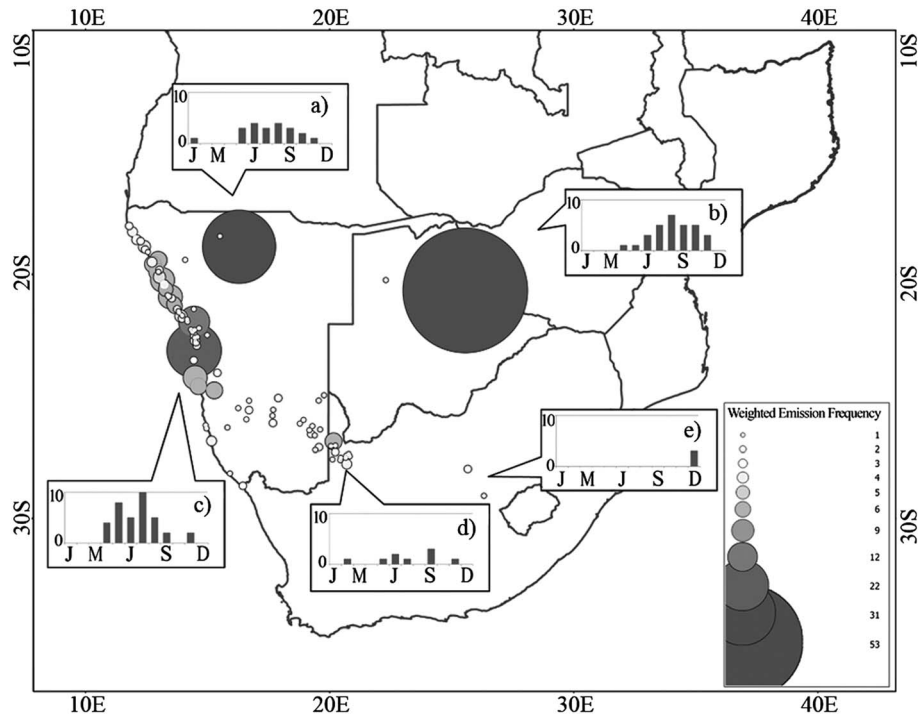


Figure 2. Southern African dust plume source locations. Plume frequency and timing for the various regions: (a) Etosha Basin, (b) Makgadikgadi Basin, (c) Namib Coastal Sources, (d) South Western Kalahari Sources, (e) Free State Sources. Circles indicate the weighted frequency of the number of dust plumes, clearly indicating the dominance of the Makgadikgadi and Etosha Pans in detected plume frequency. Sub-basin clusters can be identified in Auxiliary Figure 1. Rivers and Pans along the Namibian coastline contribute to multiple detected plumes during the 4 year period. The bar charts represent the number of days on which each region had detected dust plumes. The Etosha basin peaks in June and August, the Makgadikgadi in August, the Free State was only seen to emit in December, while the South Western Kalahari peaked in September, and the Namibian coastline in June and August.

for the appropriate treatment of dust sources within global models [Bullard *et al.*, 2011].

3.2. Temporal Considerations.

[10] From our MSG-SEVIRI data inventory, we can see that the inland basins and pan source regions (Makgadikgadi, Etosha, and the south West Kalahari) are active during the dry winter with peak plume frequency around August and September which it is consistent with observations made by Bryant [2003] and Bryant *et al.* [2007]. The Namibian coastal sources are active from April to September, seemingly driven by favorable winter Bergwinds which occur slightly earlier in the year [Eckardt *et al.*, 2001; Eckardt and Kuring, 2005].

[11] While our data focus chiefly on inventories derived from plumes detectable in daytime, some simple diurnal patterns were still apparent. For MODIS, we found that 90% (241) of plumes were identified at morning overpass (Terra), with the remaining 10% only apparent in the afternoon (Aqua) stressing the short-lived nature of events. A similar cycle was apparent for MSG. Noon images revealed the greatest number of detectable plumes, with 51% (33) of all plumes, while the 09:00 images showed 31% of the plumes (20), the remaining 18% (12 plumes) occurred at 15:00. These data help to quantify some of the spatial and temporal bias inherent in global dust source products derived from remote sensing data.

[12] The combined use of two image data sets here is not without some bias. A total of 1889 MSG images (three per

day) were analyzed which featured a total of 65 dust plumes from 23 inland sources (Supporting Figure S2). The 4486 MODIS tiles (2 tiles per day) generated the remaining 263 plumes on 56 days, attributable to 93 sources, many of them coastal. Of all MSG imagery, 2.1% depicted plumes compared to 1.3% of all MODIS imagery. A proportion of these differences can be attributed to data gaps and detection characteristic of each sensor. Twelve inland sources were detected on MSG that were not detected using the MODIS, which include the two Free State plume sources and an additional 10 sources in the south-western Kalahari Pan belt. The remaining 11 MSG-derived source locations matched well with MODIS detection and include the large Makgadikgadi and Etosha Pans as well as nine sources in the south-western Kalahari Pan belt. Along the Namibian coastline, MODIS detected 70 coastal sources which were not visible on the MSG composite due to specific limitations of the algorithm [Legrand *et al.*, 2001; Brindley *et al.*, 2012]. There was relatively close agreement between the two products for Makgadikgadi and Etosha pans, with coincidental plumes on both data sets. Coincidental detection (Supporting Figure S1 and Supporting Table S1) was limited by the retrieval of MSG data on local servers (Supporting Figure S2). The current development of improved algorithms to enhance the weak, transient dust signals in SEVIRI false color imagery forms the basis of ongoing research in this region [Banks *et al.*, 2013] which should improve event retrievals in future.

4. Conclusions

[13] Our regional source inventory for southern Africa presents 101 plume source points representing considerably more detail than the two sources determined by *Prospero et al.* [2002], to six in *Washington et al.* [2003] and more recently 10 sources by *Ginoux et al.* [2012]. This demonstrated that combined use of visually interpreted MODIS and MSG-SEVIRI data can build significantly upon prior dust observations using global TOMS, OMI and MODIS products. Our plume observations have identified sub-basin scale source clusters for the Etosha and Makgadikgadi Pans and have for the first time detected active plumes in the south western Kalahari pan belt. We can also report that more than half of all the plumes detected in southern Africa originate from pans. This figure is considerably higher than for any other previously interrogated source regions (e.g., Chihuahuan Desert, LEB, Sahara). The multitemporal observations for southern Africa also show that dust plumes are most active before noon in all source regions. Such detailed observations are crucial in guiding ground-based observations seeking to investigate controls on emission due to surface characteristics and sediment supply dynamics, as well as to inform a range of modelling activities [Bryant, 2013]. Our findings here have already guided field monitoring to emissive locations at the Makgadikgadi Pans [2011 and 2012] as well as the Huab, Kuiseb, and Tsauchab Rivers (2013) in the Namib Desert. Without significant field observations, it cannot be ascertained to what extent anthropogenic factors contribute to the emissions observed here.

[14] The manual analysis of MODIS and MSG composite data is effective, but not time efficient and certainly not devoid of user and subjectivity constraints. Our study also demonstrates [in line with *Baddock et al.*, 2009] that no single remote sensing product is currently able to provide a systematic dust source map which can pinpoint plume origin to within a few km at a continental or regional scale; and that a synergistic approach to remote sensing data and algorithm use is often appropriate [Bryant, 2013]. Further improvements to methods and retrieval approaches to aid dust source detection and characterization using both MSG-SEVIRI and MODIS form the basis of ongoing research. In general point sources, even small playas were readily identifiable in the 250 m resolution true color MODIS imagery and source attribution in MSG was more difficult if there were no coincidental plumes with MODIS. It appears that MODIS true color plumes may well be younger and lower and that MSG is better at detecting aged, elevated, and cooler plumes.

[15] **Acknowledgments.** We acknowledge the use of Rapid Response imagery from the Land Atmosphere Near-real time Capability for EOS (LANCE) system operated by the NASA/GSFC/Earth Science Data and Information System (ESDIS) with funding provided by NASA/HQ, as well as Chris Jack for the preprocessing of the MSG data from imagery stored by CSAG (Climate Systems Analysis Group), UCT. We also acknowledge the contributions of the anonymous reviewers for their constructive comments.

[16] The Editor thanks Matthew Baddock and an anonymous reviewer for their assistance in evaluating this paper.

References

Abel, S. J., E. J. Highwood, J. M. Haywood, and M. A. Stringer (2005), The direct radiative effect of biomass burning aerosols over southern Africa, *Atmos. Chem. Phys.*, *5*, 1999–2018, doi:10.5194/acp-5-1999-2005.

Ackerman, S. A. (1997), Remote sensing aerosols using satellite infrared observations, *J. Geophys. Res.*, *102*(D14), 17,069–17,079, doi:10.1029/96JD03066.

Ashpole, I., and R. Washington (2012), An automated dust detection using SEVIRI: A multiyear climatology of summertime dustiness in the central and western Sahara, *J. Geophys. Res.*, *117*, D08202, doi:10.1029/2011JD016845.

Baddock, M. C., J. E. Bullard, and R. G. Bryant (2009), Dust source identification using MODIS: A comparison of techniques applied to the Lake Eyre Basin, Australia, *Remote Sens. Environ.*, *113*(7), 1511–1523, doi:10.1016/j.rse.2009.03.002.

Banks, J. R., H. E. Brindley, C. Flamant, M. J. Garay, N. C. Hsu, O. V. Kalashnikova, L. Klüser, and A. M. Sayer (2013), Intercomparison of satellite dust retrieval products over the west African Sahara during the Fenec campaign in June 2011, *Remote Sens. Environ.*, *136*, 99–116, doi:10.1016/j.rse.2013.05.003.

Brindley, H. E., P. Knippertz, C. Ryder, and I. Ashpole (2012), A critical evaluation of the ability of the Spinning Enhanced Visible and Infrared Imager (SEVIRI) thermal infrared red-green-blue rendering to identify dust events: Theoretical analysis, *J. Geophys. Res.*, *117*, D07201, doi:10.1029/2011JD017326.

Bryant, R. G. (2003), Monitoring Hydrological Controls on dust emissions: Preliminary observations from Etosha Pan, Namibia, *Geogr. J.*, *169*(2), 131–141, doi:10.1111/1475-4959.04977.

Bryant, R. G., G. R. Bigg, N. M. Mahowald, F. D. Eckardt, and S. G. Ross (2007), Dust emission response to climate in southern Africa, *J. Geophys. Res.*, *112*, D09207, doi:10.1029/2005JD007025.

Bryant, R. G. (2013), Recent advances in our understanding of dust source emission processes, *Prog. Phys. Geogr.*, *37*(3), 397–421, doi:10.1177/0309133313479391.

Bullard, J., M. Baddock, G. H. McTainsh, and J. Leys (2008), Sub-basin scale dust source geomorphology detected using MODIS, *Geophys. Res. Lett.*, *35*, L15404, doi:10.1029/2008GL033928.

Bullard, J. E., S. P. Harrison, M. C. Baddock, N. Drake, T. E. Gill, G. McTainsh, and Y. Sun (2011), Preferential dust sources: A geomorphological classification designed for use in global dust-cycle models, *J. Geophys. Res.*, *116*, F04034, doi:10.1029/2011JF002061.

Carslaw, K. S., O. Boucher, D. V. Spracklen, G. W. Mann, J. G. L. Rae, S. Woodward, and M. Kulmala (2010), A review of natural aerosol interactions and feedbacks with the Earth system, *Atmos. Chem. Phys.*, *10*(4), 1701–1737, doi:10.5194/acp-10-1701-2010.

Eckardt, F. D., R. Washington, and J. Wilkinson (2001), The origin of dust on the West Coast of Southern Africa, *Palaeoecol. Afr.*, *27*, 207–219.

Eckardt, F. D., and N. Kuring (2005), SeaWiFS identifies dust sources in the Namib Desert, *Int. J. Remote Sens.*, *26*(19), 4159–4167, doi:10.1080/01431160500113112.

Engelstaedter, S., and R. Washington (2007), Temporal controls on global dust emissions: The role of surface gustiness, *Geophys. Res. Lett.*, *34*, L15805, doi:10.1029/2007GL029971.

Gabric, A. J., R. A. Cropp, G. H. McTainsh, B. M. Johnston, H. Butler, B. Tilbrook, and M. Keywood (2010), Australian dust storms in 2002–2003 and their impact on Southern Ocean biogeochemistry, *Global Biogeochem. Cycles*, *24*, GB2005, doi:10.1029/2009GB003541.

Ginoux, P., J. M. Prospero, T. E. Gill, N. C. Hsu, and M. Zhao (2012), Global scale attribution of anthropogenic and natural dust sources and their emission rates based on MODIS Deep Blue aerosol products, *Rev. Geophys.*, *50*, RG3005, doi:10.1029/2012RG000388.

Holmes, P. J., M. D. Bateman, D. S. G. Thomas, M. W. Telfer, C. H. Barker, and M. P. Lawson (2008), A Holocene-late Pleistocene aeolian record from lunette dunes of the western Free State panfield South Africa, *Holocene*, *18*, 1193–1205, doi:10.1177/0959683608095577.

Hsu, N. C., S. C. Tsay, and M. D. King (2004), Aerosol properties over bright-reflecting source regions, *IEEE Trans. Geosci. Remote Sens.*, *42*(3), 557–569, doi:10.1109/TGRS.2004.824067.

Hsu, N. C., S. C. Tsay, M. D. King, and J. R. Herman (2006), Deep blue retrievals of Asian aerosol properties during ACE-Asia, *IEEE Trans. Geosci. Remote Sens.*, *44*(11), 3180–3195, doi:10.1109/TGRS.2006.879540.

Ichoku, C., L. A. Remer, Y. J. Kaufman, R. Levy, M. A. Chu, D. Tanre, and B. N. Holben (2003), MODIS observation of aerosols and estimation of aerosol radiative forcing over southern Africa during SAFARI 2000, *J. Geophys. Res.*, *108*(D13), 8499, doi:10.1029/2002JD002366.

Knippertz, P., and M. C. Todd (2012), Mineral dust aerosols over the Sahara: Meteorological controls on emission and transport and implications for modeling, *Rev. Geophys.*, *50*, RG1007, doi:10.1029/2011RG000362.

Kohlfeld, K. E., and I. Tegen (2007), The record of soil dust aerosols and their role in the earth system, in *Treatise on Geochemistry*, vol. 1, edited by H. D. Holland and K. K. Turekian, pp. 1–26, Elsevier Ltd., Oxford.

Kok, J. F. (2011), A scaling theory for the size distribution of emitted dust aerosols suggests climate models underestimate the size of the global dust cycle, *Proc. Natl. Acad. Sci. U. S. A.*, *108*(3), 1016–1021, doi:10.1073/pnas.1014798108.

Lee, J. E., T. E. Gill, K. R. Mulligan, M. D. Acosta, and A. E. Perez (2009), Land use/land cover and point sources of the 15 December 2003 dust

- storm in southwestern North America, *Geomorphology*, 105(1-2), 18–27, doi:10.1016/j.geomorph.2007.12.016.
- Legrand, M., A. Plana-Fattori, and C. N'Doume (2001), Satellite detection of dust using the IR imagery of Meteosat 1. Infrared difference dust index, *J. Geophys. Res.*, 106(D16), 18,251–18,275, doi:10.1029/2000JD900749.
- Maenhaut, W., J. Schwarz, J. Cafmeyer, and H. J. Annegarn (2002), Study of elemental mass size distributions at Skakuzu, South Africa, during the SAFARI 2000 dry season campaign, *Nucl. Instrum. Methods Phys. Res., Sect. B*, 189, 254–258, doi:10.1016/S0168-583X(01)01053-9.
- Mahowald, N. (2011), Aerosol indirect effect on biogeochemical cycles and climate, *Science*, 334(6057), 794–796, doi:10.1126/science.1207374.
- Mahowald, N. M., J. A. Ballantine, J. Feddema, and N. Ramankutty (2007), Global trends in visibility: Implications for dust sources, *Atmos. Chem. Phys.*, 7(12), 3309–3339, doi:10.5194/acp-7-3309-2007.
- Mahowald, N. M., S. Engelstaedter, C. Luo, A. Sealy, P. Artaxo, C. Benitez-Nelson, S. Bonnet, Y. Chen, P. Y. Chuang, and D. D. Cohen (2009), Atmospheric iron deposition: Global distribution, variability, and human perturbations, *Ann. Rev. Mar. Sci.*, 1, 245–278, doi:10.1146/annurev.marine.010908.163727.
- Mahowald, N. M., D. S. Ward, S. Kloster, M. G. Flanner, C. L. Heald, N. G. Heavens, P. G. Hess, J. Lamarque, and P. Y. Chuang (2011), Aerosol impacts on climate and biogeochemistry, *Annu. Rev. Environ. Resour.*, 36(1), 45–74.
- Okin, G. S., J. E. Bullard, R. L. Reynolds, J. A. Ballantine, K. Schepanski, M. C. Todd, J. Belnap, M. C. Baddock, T. E. Gill, and M. E. Miller (2011), Dust: Small-scale processes with global consequences, *EOS, Trans. Am. Geophys. Union*, 92, 241–248, doi:10.1029/2011EO290001.
- Piketh, S. J., H. J. Annegarn, and P. D. Tyson (1999), Lower Tropospheric aerosol dust loadings over South Africa: The relative contribution of aeolian dust industrial emissions and biomass burning, *J. Geophys. Res.*, 104, 1597–1607, doi:10.1029/1998JD100014.
- Prospero, J. M. (1999), Long-range transport of mineral dust in the global atmosphere: Impact of African dust on the environment of the south eastern United States, *Proc. Natl. Acad. Sci. U. S. A.*, 96, 3396–3403, doi:10.1073/pnas.96.7.3396.
- Prospero, J. M., P. Ginoux, O. Torres, S. E. Nicholson, and T. E. Gill (2002), Environmental characterization of global sources of atmospheric dust identified with the nimbus 7 Total Ozone Mapping Spectrometer (TOMS) absorbing aerosol product, *Rev. Geophys.*, 40(1), 1002, doi:10.1029/2000RG000095.
- Ravi, S., et al. (2011), Aeolian processes and the biosphere, *Rev. Geophys.*, 49, RG3001, doi:10.1029/2010RG000328.
- Rivera Rivera, N. I., T. E. Gill, M. P. Bleiweiss, and J. L. Hand (2010), Source characteristics of hazardous Chihuahuan Desert dust outbreaks, *Atmos. Environ.*, 44, 2457–2468, doi:10.1016/j.atmosenv.2010.03.019.
- Schepanski, K., I. Tegen, B. Laurent, B. Heinold, and A. Macke (2007), A new Saharan dust source activation frequency map derived from MSG-SEVIRI IRchannels, *Geophys. Res. Lett.*, 34, L18803, doi:10.1029/2007GL030168.
- Schulz, M., et al. (2012), Atmospheric transport and deposition of mineral dust to the ocean: Implications for research needs, *Environ. Sci. Tech.*, 46(19), 10,390–10,404, doi:10.1021/es300073u.
- Shao, Y., K. H. Wyrwoll, A. Chappell, J. Huang, Z. Lin, G. H. McTainsh, M. Mikami, T. Y. Tanaka, X. Wang, and S. Yoon (2011), Dust cycle: An emerging core theme in Earth system science, *Aeolian Res.*, 2(4), 181–204, doi:10.1016/j.aeolia.2011.02.001.
- Skiles, S. M., T. H. Painter, J. S. Deems, A. C. Bryant, and C. Landry (2012), Dust radiative forcing in snow of the Upper Colorado River Basin: Part II. Interannual variability in radiative forcing and snowmelt rates, *Water Resour. Res.*, 48, W07522, doi:10.1029/2012WR011986.
- Vickery, K. J., and F. D. Eckardt (2013), Dust emission controls on the lower Kuiseb River valley, Central Namib, *Aeolian Res.*, 10, 125–133, doi:10.1016/j.aeolia.2013.02.006.
- Washington, R., M. C. Todd, N. J. Middleton, and A. S. Goudie (2003), Dust-Storm source areas determined by the Total Ozone Monitoring Spectrometer and Surface Observations, *Ann. Assoc. Am. Geogr.*, 93(2), 297–313, doi:10.1111/1467-8306.9302003.
- Washington, R., C. Bouet, G. Cautenet, E. Mackenzie, I. Ashpole, S. Engelstaedter, G. Lizcano, G. M. Henderson, K. Schepanski, and I. Tegen (2009), Dust as a tipping element: The Bodélé Depression, Chad, *Proc. Natl. Acad. Sci.*, 106(49), 20,564–20,571, doi:10.1073/pnas.0711850106.
- Zender, C. S., H. Bian, and D. Newman (2003), Mineral Dust Entrainment and Deposition (DEAD) model: Description and 1990s dust climatology, *J. Geophys. Res.*, 108(D14), 4416, doi:10.1029/2002JD002775.